

NATIONAL ADVISORY COMMITTEE FOR AERONAUTICS

WARTIME REPORT

ORIGINALLY ISSUED
July 1941 as
Advance Confidential Report

THE EFFECT OF EXTERNAL SHAPE UPON THE DRAG OF A SCOOP

By Irven Naiman and Paul R. Hill

Langley Memorial Aeronautical Laboratory
Langley Field, Va.



WASHINGTON

NACA WARTIME REPORTS are reprints of papers originally issued to provide rapid distribution of advance research results to an authorized group requiring them for the war effort. They were previously held under a security status but are now unclassified. Some of these reports were not technically edited. All have been reproduced without change in order to expedite general distribution.

THE EFFECT OF EXTERNAL SHAPE UPON THE DRAG OF A SCOOP

By Irven Naiman and Paul R. Hill

SUMMARY

The principles of NACA cowling design may be applied to scoop fairing. Six scoops were built and tested to show the advantage of using these principles. Three of the scoops had a good nose contour with different afterbody lengths, and three were of inferior nose shape.

The best scoop tested increased the drag coefficient of the airplane by 0.0013, although its frontal area was over one-fifth that of the fuselage. The critical speed with the best nose tested was 400 miles per hour. The poorest scoop, with same entrance area but smaller frontal area, practically doubled the drag of the airplane.

The drag with long afterbodies was found to be fairly insensitive to large changes in length. The longest afterbody tested, with a length of eleven times its depth, appeared to be most favorable.

An appendix gives a method of obtaining the dimensions of a scoop that will give the lowest drag for a given application. In the determination of these dimensions the power cost of frontal area is balanced against the power cost of internal expansion losses. The analysis shows that a low form drag scoop with low velocity entrance gives the best practical compromise.

INTRODUCTION

In the past, airplanes have been designed with a great many scoops upon the surface; some have fairly bristled with scoops. It is generally realized today that these protuberances are a source of considerable drag and that the number and size should therefore be reduced as much as possible. While the most efficient way to take in the cooling and engine air required by an airplane is at the front stagnation point (fuselage or nacelle), in many air-cooled engine installations, due to inadequate frontal opening, additional air must be brought in through scoops

for auxiliaries such as intercoolers and oil coolers. It is also current practice on most liquid-cooled engine installations to house the glycol and oil coolers in a duct under the fuselage or nacelle. The present investigation was undertaken to determine the cost of a scoop installation on which the principles of the NACA cowling (reference 1) had been applied. These principles include a nose shape of sufficient curvature so that breakaway does not occur over the lip of the duct at any flight attitude, and an entrance large enough to insure small internal expansion loss. There are presented herein several designs of ducts in which the nose and afterbody shapes were varied.

APPARATUS AND TESTS

The scoop tests were made on a 0.4-scale model of the XP-41 airplane with a revised fuselage 25 percent longer than the original one. The model included canopy and open-nose cowling with air flow, but no tail surfaces. It was assumed that tail surfaces would have no effect on the tests.

The tests were run in the 19-foot pressure tunnel at a dynamic pressure of 50 pounds per square foot and at a Reynolds number of approximately 3×10^6 based on the mean wing chord. The model was supported on the usual airfoil supports and on a special tail support having a high fineness ratio to minimize buoyancy effects. Lift and drag measurements were made over an angle-of-attack range from -2° to 20° .

Six scoops, designated A to F, were tested on the bottom of the fuselage. The layout of the test arrangements showing the contours of these scoops is given in figures 1 and 2. All of the scoops had the same area of nose opening, approximately 47 square inches. Scoops A to D have well-rounded noses, increasing the projected frontal area to 113 square inches. (The projected fuselage frontal area is 502 square inches.) These scoops increase the over-all depth of the fuselage $7\frac{1}{4}$ inches. This large size was used in order to obtain accuracy in testing. Scoops A to C have the same nose with afterbodies of successively decreasing lengths (fig. 1). The nose contours may be seen in figure 3. As the nose contour approaches the intersection with the fuselage all radii of curvature greatly increase. A streamline nose is also pro-

L-331

vided and was tried on scoop A (fig. 1). The afterbodies are tapered mostly in depth and very little in width. Scoop A was provided with an exit slot 10 inches long and widths of 0.3 inch, 0.6 inch, and a 30° flap opening to 1.7 inches (figs. 1, 4, and 5). The exits for scoops B and C were obtained by an alternate tail with the end cut off (fig. 6).

Scoop D (figs. 6 and 7) has the medium afterbody of B, but has a sharp-edge nose resulting from a simple sheet-metal construction. However, the longitudinal contours of the nose-lip are well rounded on both the bottom and sides.

Scoop D₁ is the same as scoop D except that a strip of metal is cut from the side of the scoop nose. This strip tapers from nothing at the corner of the scoop to 1 inch at the intersection with the fuselage (fig. 2). Scoop D₂ is similar except that the strip tapers from nothing to 2 inches. The scoop nose was trimmed back to see what drag penalty is imposed by decreasing the nose radius at the intersection with the fuselage.

Scoop E (figs. 2 and 8) has straight sides, so that the maximum area is the same as that of the nose opening. Scoop F is approximately conical in shape with a ratio of length to depth of 3. It was designed to test the form drag only, having no exit passage to provide for air flow.

The noses of scoops A to F were directly below the leading edge of the wing. Scoop D was also tried with its nose 8 inches behind the leading edge to see if the proximity of the wing had any stabilizing effect on the flow over the scoop. In this position it is designated D_x.

A baffle plate with twenty 1-inch holes (conductance area = 10.2 sq in.) obstructed the internal air flow for scoops A, B, C, and D. Scoop E had no baffle plate and scoop F was not tested with air flow.

The additional drag due to the cooling air (reference 1) is given by

$$\Delta C_D' = \frac{KF}{S} \left(\frac{\Delta p}{q} \right)^{3/2}$$

For this model with KF = 10.2 sq in., this equation becomes

$$\Delta C_D' = 0.002 \left(\frac{\Delta p}{\rho} \right)^{3/2}$$

Pitot and static pressure measurements were made to determine the total pressure in the nose, the pressure drop across the baffle, and the velocity in the exit. In the nose of scoop A, three rows of surface static pressure orifices were installed to determine the pressure distribution along the surface. These were located on the bottom center line, on the corner where the scoop turned upward, and in the fillet at the body juncture, and are designated a, b, and c, respectively, in figure 3.

SYMBOLS

- A conductance area of baffle
- A_1 area of entrance
- A_2 area of exit
- c mean aerodynamic chord of wing, 2.49 feet
- c loss coefficient due to angle of expansion
- C_D drag coefficient ($D/q_c S$)
- ΔC_D increase in drag coefficient caused by scoop
- $\Delta C_D'$ calculated increase in drag coefficient caused by air flow
- C_f drag coefficient of scoop, based on its frontal area
- C_L lift coefficient ($L/q_c S$)
- C_m pitching-moment coefficient ($M/q_c c S$)
- D drag force
- F area of duct at baffle plate
- k ratio of scoop frontal area to entrance area
- K conductance of baffle plate (A/F)

K_1	conductance of entrance	$\left(\frac{1}{\sqrt{c} \left(\frac{F}{A_1} - 1 \right)} \right)$
K_2	conductance of exit	(A_2/F)
L	lift force	
M	moment about quarter-chord point	
M	Mach number	
p	static pressure on surface, referred to static pressure of air stream	
p_f	total pressure in front of baffle plate, referred to static pressure of air stream	
p_r	total pressure in rear of baffle plate, referred to static pressure of air stream	
p_e	static pressure at exit, referred to static pressure of air stream.	
Δp	pressure drop across baffle	$(p_f - p_r)$
Δp_1	pressure drop in entrance	
Δp_2	pressure drop in exit	
ΔP	over-all pressure difference when no air is flowing	
q_c	impact pressure of air stream, referred to static pressure of air stream	$[1/2 \rho V^2 (1 + 1/4 M^2 + \dots)]$
q_F	dynamic pressure in duct	$(1/2 \rho V_F^2)$
Q	quantity of air flow	
S	wing area, 35.8 square feet	
V	velocity of air stream	
V_1	velocity in entrance	(Q/A_1)
V_2	velocity in exit	(Q/A_2)
V_F	velocity in duct at baffle plate	(Q/F)

- α angle of attack
- ρ mass density of air stream

RESULTS AND DISCUSSION

Drag.- The lift, drag, and pitching-moment coefficients as functions of angle of attack are given in figures 9 and 10 for the basic model and the model with scoop B with air flow, respectively. Figure 11 gives the drag coefficient C_D for the various test arrangements plotted in polar form as a function of the lift coefficient C_L up to $C_L = 0.4$. At the lift coefficient corresponding to high-speed flight, 0.117, table I gives the drag coefficient and the increment ΔC_D over the basic drag.

The drag coefficient of the model in the basic condition is 0.0138. Deducting the induced drag and the profile drag of the exposed portion of the wing, as given in reference 2, the fuselage drag may be taken as 0.0060. The addition of scoop A increased the frontal area by 22.5 percent. The expected drag increase is thus 0.0013, the value actually obtained for scoop A with the streamline nose (run 2). When the blunt nose is used, however, the drag is increased slightly. Scoops A, B, C, and D_x each add a drag increment of 0.0017 and scoop D, 0.0019. The differences between these drag values are not significant, being within the experimental error, and it appears that there was no particular stabilizing effect due to the pressure gradient at the leading edge of the wing. The drag of the blunt nose at zero air flow is not the true measure, for the bluntness is present to accommodate air flow. In several cases the opening of the exit to allow air flow reduced the drag, though never below the basic value of 0.0013. Inasmuch as the calculated cooling drag increment at maximum air flow is only 0.0002, approximately the experimental error, the scoop drag increments with cooling air should be 0.0015 ± 0.0002 . The results in table I are therefore considered a very good check, and indicate that an external scoop installation for an oil cooler or intercooler can be made at low cost.

Scoops E and F were tested to show that an attempt to limit the frontal area of the scoop to the inlet area results in very high drag increments because of the poor nose

shape. Scoop E with a drag increment of 0.0085 has five times the drag of scoop B, and scoop F with 0.0137 has eight times the drag of scoop B, almost doubling the model drag. Scoops D_1 and D_2 (scoop D with cuts made at the juncture) further illustrate the necessity for good flow over the leading edge of the scoop. Scoop D_2 almost doubled the drag of scoop D.

Cooling pressure.- The pressure readings at various places in the entrance of the scoop, behind the baffle, and in the exit are given as fractions of the dynamic pressure in tables II and III. There is a considerable variation in the value of this pressure at the several locations in the entrance. The boundary layer at the surface of the fuselage causes a lower pressure at the top of the scoop than at the bottom. Because of this pressure difference there is set up a swirl or cross flow in the entrance, such that the air enters along the central and bottom portions of the scoop, passes toward the baffle, turns upward, comes forward along the top of the entrance, and spills out along the fillet. Because of this flow pattern, the survey tubes are not aligned with the local flow, giving an erroneous pressure reading. It is for this reason that the front pressures appear to be such a small proportion of the stream q . Table III shows that at high rates of air flow (which tend to eliminate the swirl pattern) the front pressure readings come almost to stream q . At high angles of attack, the air flows obliquely across the fuselage, reducing the boundary layer underneath the fuselage. This smaller boundary layer reduces the cross flow in the scoop entrance, resulting in a higher value of the front pressure.

The swirl in the entrance is an undesirable feature from the standpoint of cooling, and an attempt should be made to eliminate the effect of the boundary layer by a plate separating the high and low energy air.

With air flow the pressure drop across the baffle is given in table III. The pressure drop was taken as the difference between the baffle pressure and the rear pressure. The static pressure in the exit is omitted for scoop A because of faulty measurements. The exit area was apparently too small for adequate air flow with scoop A. However, the effect of the flap in increasing the pressure drop is notable. For the larger baffle conductance approximately $0.7q$ was obtained. It is realized that the drag increase with flap was expensive from the standpoint of drag, but in the take-off and climb it is the cooling that is all important.

Surface pressure survey.— Observation of the pressure distribution over the nose of scoop A was made without internal air flow. This condition gives the maximum external velocities and therefore the most severe surface pressure conditions. Surface pressures are presented for angles of attack of 1.1° and 8.7° , representing the high-speed and climb conditions. The maximum negative pressure on the scoop nose occurs at the lowest angle of attack. Figure 12 shows that for an angle of attack of 1.1° the maximum negative p/q is 1.6, occurring on the center line of the scoop. This value of p/q corresponds to a critical speed of 420 miles per hour at sea level and 395 miles per hour at 20,000 feet altitude. By reducing the curvature at the point of maximum negative pressure, the velocity at this point can be reduced, thereby increasing the critical speed. In this manner a contour may be obtained satisfactory for any desired design speed.

CONCLUDING REMARKS

The most desirable place to take in cooling air for accessories, such as oil coolers, intercoolers, etc., is at the nose of the fuselage or nacelle, even if it is necessary to increase the cowling area. However, if it is necessary to take air in through a scoop or underslung duct, low scoop drag may be secured by utilizing the design principles of the NACA cowling. This design involves the use of well-rounded nose contours, thus giving a frontal area much larger than the inlet area. Scoops tested with this type of nose gave not only a low drag increase but a critical speed of 400 miles per hour with no air flow.

Scoop drag was found to be quite insensitive to changes in afterbody length in the range of four to eleven times the scoop depth. However, with air flow, the drag decreased slightly with increasing length, the lowest value being obtained with scoop A. This scoop was of such length that it practically merged into the body without a break in the contour lines. Complete disregard of the principles of fairing resulted in a scoop which almost doubled the drag of the model.

Langley Memorial Aeronautical Laboratory,
National Advisory Committee for Aeronautics,
Langley Field, Va..

APPENDIX

Analysis of Scoop Design

The results of this study may be incorporated into the known principles of scoop design. The design of a scoop may be divided into two parts: the design of the duct and the design of the external shape.

The duct.— The duct consists of an entrance area, an expansion region, the working region, and the exhaust region. For a carburetor duct the carburetor is the working region and there is no exhaust region to be considered. The working region is the one in which the oil cooler, prestone cooler, intercooler, or air-cooled engine is placed. The cooling specifications for this region include a certain quantity of air flow Q at a certain altitude (determining the air density ρ). The heat exchanger has a frontal area F and its internal resistance is such that a pressure difference Δp is required to secure the required quantity of air flow. These elements may all be included in one quantity, the conductance, given by

$$K = \frac{Q}{F} \sqrt{\frac{\rho}{2\Delta p}} \quad (1)$$

or

$$K^2 = \frac{\frac{1}{2} \rho \left(\frac{Q}{F}\right)^2}{\Delta p} = \frac{\frac{1}{2} \rho V_F^2}{\Delta p} = \frac{q_F}{\Delta p} \quad (2)$$

where $V_F = Q/F$ and q_F is the dynamic pressure in the duct at the heat exchanger. For oil and prestone coolers K is approximately 0.5, for intercoolers 0.2 to 0.3, depending upon design. Tightly baffled air-cooled engines vary from 0.10 to 0.18 depending upon the number of cylinders; loosely baffled engines may be as high as 0.5.

The over-all pressure difference ΔP is equal to the difference between the total pressure at the entrance to the duct system and the static pressure at the exit. In addition to the pressure loss Δp across the heat exchanger, there is an additional loss Δp_1 due to expansion in the entrance. Δp_1 and Δp are total pressure losses and appear as drag of the cooling system. The pressure

difference remaining after deducting Δp_1 and Δp from ΔP is the difference between the total pressure in the exit passage and the static pressure at the exit. This pressure difference may be designated Δp_2 and is, of course, equal to the dynamic pressure of the air at the exit. The pressure equation is thus given as

$$\Delta P = \Delta p_1 + \Delta p + \Delta p_2 \quad (3)$$

If the duct system is very long, a further allowance will have to be made for friction and bend losses.

Inasmuch as the entrance loss Δp_1 is a total pressure loss, whereas Δp_2 is the dynamic pressure of the exit air, it is seen that any throttling of the flow should occur by constriction of the exit. Throttling in the entrance region can be accomplished only by pressure loss with a consequent increase in drag.

Entrance and exit conductances may be defined in a manner similar to equation (2).

$$K_1^2 = q_F / \Delta p_1 \quad (4)$$

$$K_2^2 = q_F / \Delta p_2 \quad (5)$$

Equation (3) may be rewritten as

$$\begin{aligned} \frac{\Delta P}{\Delta p} &= 1 + \frac{\Delta p_1}{\Delta p} + \frac{\Delta p_2}{\Delta p} \\ &= 1 + \left(\frac{K}{K_1} \right)^2 + \left(\frac{K}{K_2} \right)^2 \end{aligned} \quad (6)$$

In order to secure the proper apportionment of the over-all pressure ΔP , it is thus necessary to make K_1 as large as practicable (to reduce the entrance loss) and to make K_2 as small as is necessary to balance the equation.

The entrance conductance K_1 may be determined as follows. The expansion loss in the entrance region in passing from an area A_1 to an area F is given by

$$\Delta p_1 = c \frac{1}{2} \rho V_1^2 \left(1 - \frac{A_1}{F} \right)^2$$

Upon substituting $A_1 V_1 = F V_F$, then

$$\begin{aligned} \Delta p_1 &= c \frac{1}{2} \rho V_F^2 \left(\frac{F}{A_1} - 1 \right)^2 \\ &= c q_F \left(\frac{F}{A_1} - 1 \right)^2 \end{aligned}$$

where c is a factor dependent upon the angles of divergence of the walls (fig. 13) (reference 2), and V_1 is the velocity at A_1 , and V_F is the velocity at F . Then

$$\frac{1}{K_1^2} = \frac{\Delta p_1}{q_F} = c \left(\frac{F}{A_1} - 1 \right)^2 \quad (7)$$

This function is given in figure 14. The range of c is from 0.13 to 1.21 approximately 1:10; that is, the worst internal expansion will have ten times the entrance loss that a perfect one would have. The effect of an expansion angle larger than the optimum can be easily compensated by increasing the entrance area somewhat. (See fig. 14.) Thus, an opening only slightly larger than the minimum will permit a short entrance length.

From equations (2) and (4)

$$\frac{1}{K_1^2} = \frac{\Delta p_1}{K^2 \Delta p}$$

Thus, with K and Δp specified, selection of Δp_1 determines K_1 . Conversely, if the geometric design is selected, Δp_1 is determined. For example, for a radiator with a required pressure drop of 40 pounds per square foot $K^2 \Delta p = 10$ pounds per square foot. If the entrance area is 0.45 F , the entrance loss is between 2 and 18 pounds per square foot. An increase of area to 0.55 F sets a loss of 8 pounds per square foot as an upper limit with 3 or 4 as a more probable value.

The problem of the permissible entrance loss is tied up with the problem of securing adequate air flow in the climb conditions. Because of the low air speed the entrance

loss must be made small. The over-all pressure difference may be improved by placing the entrance and exit in the propeller slipstream. By fitting a flap to the exit under these conditions, over-all pressure differences four or five times the dynamic pressure may be obtained (reference 3).

The exit conductance K_2 may be determined as follows:

$$\begin{aligned}\Delta p_2 &= \frac{1}{2} \rho V_2^2 \\ &= \frac{1}{2} \rho V_F^2 \left(\frac{V_2}{V_F} \right)^2 \\ &= q_F \left(\frac{F}{A_2} \right)^2\end{aligned}$$

for $FV_F = A_2V_2$. The exit conductance is thus given as

$$K_2^2 = q_F / \Delta p_2 = (A_2 / F)^2$$

or

$$K_2 = A_2 / F \quad (8)$$

An exact method of determining the dimensions of A_2 for all flow conditions is rather difficult. However, two general rules may be used as a first estimate: (1) If $\Delta p_2 > 0.5q$, the minimum area of the exit perpendicular to the flow lines out of the slot is a good estimation. (2) If $\Delta p_2 < 0.5q$, an area larger than that computed by the above formula will have to be used since the velocity distribution across the slot is not uniform.

External design.— The flow pattern of the air approaching the entrance determines the external design of the scoop. If the entrance velocity approximately equals stream velocity the streamlines will be nearly straight. A sharp leading edge would be permissible under these conditions. When the ratio of entrance velocity to stream velocity is low, the streamlines turn sharply outward and after passing the edge of the scoop entrance must again turn through approximately 90° to resume their original direction. This low ratio is usually the condition with high flight speeds, since the upper limit of this ratio

is determined by the cooling requirement in climb. A well-rounded nose contour is necessary to prevent the occurrence of high negative pressures with attendant compressibility and separation losses. This design, of course, necessitates a projected frontal area much larger than the intake opening in order to secure the proper fairing. Just as in the case of the NACA cowl, the radius of curvature of the longitudinal nose contours should gradually increase toward the rear to avoid a sudden decrease of negative pressure.

Afterbodies must be of sufficient length to prevent the occurrence of separation. An estimate of the proper length may be obtained from the test results. It may be well to completely merge the afterbody into the rest of the airplane.

Although the proper entrance size will probably be determined while designing the duct, it is of interest to know the entrance area or scoop size which will make the sum of the internal and external drag a minimum in cruising or high-speed flight. This may be found if the form drag coefficient based on frontal area C_f is known for the particular shape of the scoop. The frontal area may be considered to be the maximum section area bounded by the scoop and the original lines of the airplane. The scoop drag is equal to the form drag plus the drag chargeable to internal flow losses. Expressing the frontal area as a coefficient times the entrance area kA_1 the drag equation is

$$D = C_{f1} k A_1 + c_{qf} \left(\frac{F}{A_1} - 1 \right)^2 \frac{Q}{V} + \frac{Q \Delta p}{V} + \dots$$

The rate of air flow Q and maximum duct area F will be considered as fixed quantities. Differentiating with respect to the entrance area, we obtain the relation for minimum drag:

$$k C_f + C_f A_1 \frac{dk}{dA_1} - 2c \left(\frac{Q}{FV} \right)^3 \left(\frac{F}{A_1} \right)^2 \left(\frac{F}{A_1} - 1 \right) = 0$$

The value of $\frac{dk}{dA_1}$ is unknown except for the case where the scoop fairing remains geometrically similar with changing size. Here $\frac{dk}{dA_1} = 0$ and the second term drops out.

If, in addition, we substitute $K \sqrt{\frac{\Delta p}{q}}$ for $\frac{Q}{FV}$, the equation takes the form

$$kC_f - 2cK^3 \left(\frac{\Delta p}{q} \right)^{3/2} \left(\frac{F}{A_1} \right)^2 \left(\frac{F}{A_1} - 1 \right) = 0$$

Design Illustrations

The application of the above formulas to the design of a low drag scoop is illustrated in table IV. The optimum scoop design is obtained when the sum of the power loss due to external drag and the power loss due to the internal expansion is a minimum. If the form drag of the scoop is large, it is best to decrease the frontal area at the expense of increasing the internal expansion loss; while, if the form drag is low, a small internal loss gives the best design. If the internal expansion loss can be kept small by perfect expansion ducts, high velocity entrances may be used; but the amount to be gained by improving the internal expansion loss is very small if a low form drag scoop is used in the design. The above observations lead us to select a scoop that has low form drag and a low velocity entrance.

The table is constructed for a flight speed of 400 miles per hour and an altitude of 20,000 feet. Rates of flow are determined for an intercooler with a conductivity of 0.2 and a required pressure drop of 60 pounds per square foot, and for a radiator with a conductivity of 0.5 and a pressure drop of 40 pounds per square foot. The expansion coefficient to be used depends on the angle of divergence between the duct walls and consequently on the distance between the scoop entrance and the heat exchanger. For a round duct with an angle of divergence of $5\frac{1}{2}^\circ$, figure 13 gives a loss coefficient of 0.13. A great duct length would be necessary to install such a duct for usual values of A_1 and $\frac{A_1}{F}$. Also, expanding ducts are usually neither round nor straight. The value of $c = 0.13$ is used in the table to represent a limiting condition rather than one to be attained. The value of $c = 1.0$ represents a sudden expansion.

The form drag coefficient based on the scoop frontal area, C_f , depends on how well the scoop is faired and how much frontal area it adds to the body on which it is placed. The lowest value obtainable is the increase due to creating a nose opening in a streamline body without increasing the frontal area. Reference 4 gives a value of $C_f = 0.008$ for this case. This value may be regarded

L-331
merely as a lower limit for an entrance located approximately at the forward stagnation point. For a well faired scoop placed so that the frontal area of the airplane is increased by an amount equal to the frontal area of the scoop, a value of $C_f = 0.059$ obtained with scoop A may be used. The values of $C_f = 0.79$ and $C_f = 1.5$ obtained with scoops E and F are included to show the effects of high form drag.

The ratio of projected frontal area to entrance area, k , is determined from the fairing layout. Its value, of course, depends on whether the scoop is faired for a low- or a high-speed entrance. Values of 1.0 and 2.4, corresponding to the scoops tested, are used in the table.

Column 7 of table IV is computed from the relation

$$\frac{Q}{F} = KV \sqrt{\frac{\Delta p}{q}}$$

Rearranging the equation for minimum drag by putting all known constants on the right side gives

$$\left(\frac{F}{A_1} - 1\right) \left(\frac{F}{A_1}\right)^2 = \frac{kC_f}{2cK^3 \left(\frac{\Delta p}{q}\right)^{3/2}}$$

The solution for $\frac{A_1}{F}$ may be obtained from figure 15 and is given in column 8. The best entrance velocity, given in column 9, equals $\left(\frac{Q}{F} / \frac{A_1}{F}\right) \frac{60}{88}$.

The external form drag and the internal expansion loss may be expressed as a parasite drag coefficient based on wing area.

$$kC_f \left(\frac{A_1}{F}\right) \left(\frac{F}{S}\right) + cK^3 \left(\frac{\Delta p}{q}\right)^{3/2} \left(\frac{F}{A_1} - 1\right)^2 \frac{F}{S} = C_{D_p}$$

The first term represents the form drag, the second the expansion loss, and C_{D_p} their sum. Numerical values

computed for $F = 2.5$ square feet and a wing area of 300 square feet are given in columns 11, 12, and 13.

Table IV shows the shift of the optimum entrance area and velocity with change in C_f . In examples 1 to 4, as C_f decreases from 1.5 to 0.008, the optimum $\frac{A_1}{F}$ increases from 0.112 to 0.414; $\frac{V_1}{V}$, varying inversely with $\frac{A_1}{F}$, drops from 0.94 to 0.25. This means that, as the form drag is decreased, it is most efficient to lower the internal loss by increasing the size of the scoop.

The effect of changing c from 1.0 to 0.13, as in examples 5 to 8, is approximately to cut the optimum $\frac{A_1}{F}$ in half and double $\frac{V_1}{V}$. In examples 9 to 16, the conditions chosen for the radiator approximately doubled the air flow; $\frac{A_1}{F}$ varies nearly as $\frac{Q}{F}$ or is nearly doubled; $\frac{V_1}{V}$ is almost unchanged.

It may be observed that the parasite drag coefficient C_{D_p} has the same trend as the form drag coefficient C_f . In examples 1 to 4, as C_f is reduced from 1.5 to 0.008, C_{D_p} drops from 0.0029 to 0.0001.

Reducing c from 1.0 to 0.13 by introducing a gradual expansion is shown in examples 5 to 8 to reduce C_{D_p} over 40 percent. However, in comparing examples 4 and 8, this reduction is too insignificant to show in the fourth decimal place. Example 4 with $\frac{V_1}{V} = 0.25$ is similar to the open-nose cowling. Evidently, with this low entrance velocity it is immaterial whether a sudden or a gradual expansion is used. On the other hand, with a high entrance velocity a gradual expansion must be used and the utmost care must be taken with duct design to prevent excessive losses. Irregularities in the entrance region easily upset the flow, and an ideal expansion is thus difficult to realize in practice. If the design calls for a small entrance and ideal expansion is not realized, the internal loss will be much greater than the external drag saving. It is therefore desirable to use as good an expansion as convenient and to use an expansion coefficient of unity in the design computations.

It is always necessary to compare the internal pres-

sure drops with the over-all pressure drop available for all flight conditions. This comparison may demand the use of a scoop larger than optimum.

CONCLUDING REMARKS

The illustrations show that the optimum scoop is determined by a compromise between the power losses associated with external drag and internal losses so that the sum of these losses is a minimum. Obviously, if the scoop has a large form drag, the size will be reduced and the internal losses will be increased to obtain the best compromise. Conversely, if the scoop has a low form drag, the frontal area will be made relatively large thereby reducing the internal losses to give the best compromise.

In the latter condition involving the scoop having low form drag, a trivial reduction in power can be obtained by reducing the frontal area due to employing ducts having ideal expansions. However, the experience and knowledge required to obtain this trivial gain are out of all proportion to the advantage to be obtained.

REFERENCES

1. Theodorsen, Theodore, Brevoort, M. J., and Stickle, George W.: Full-Scale Tests of N.A.C.A. Cowlings. NACA Rep. No. 592, 1937.
2. O'Brien, Morrrough P., and Hickox, George H.: Applied Fluid Mechanics. McGraw-Hill Book Co., 1st ed., 1937.
3. Stickle, George W., Naiman, Irven, and Crigler, John L.: Pressure Available for Cooling with Cowling Flaps. NACA Rep. No. 720, 1941.
4. Stickle, George W., Crigler, John L., and Naiman, Irven: The Effect of Streamlining the Afterbody of an N.A.C.A. Cowling. NACA ACR, Dec. 1939.

TABLE I.-- DRAG AND DRAG INCREMENT FOR THE TEST ARRANGEMENTS

$$[C_L = 0.117]$$

Run	Scoop	C_D	ΔC_D	C_f	Condition
1	-	0.0138	-----	-----	Basic: Airplane with open nose and air flow, no tail.
2	A	.0151	0.0013	0.059	Streamline nose on scoop; exit closed.
3	A	.0155	.0017	.078	A = 5.5 sq in.; $A_2 = 0$
4	A	.0151	.0013	.059	A = 5.5 sq in.; $A_2 = 3$ sq in.
5	A	.0153	.0015	.068	A = 5.5 sq in.; $A_2 = 6$ sq in.
6	A	.0195	.0057	.260	A = 5.5 sq in.; $A_2 = 17$ sq in.; 30° flap.
7	A	.0153	.0015	.068	A = 11.0 sq in.; $A_2 = 3$ sq in.
8	A	.0156	.0018	.083	A = 11.0 sq in.; $A_2 = 6$ sq in.
9	A	.0199	.0061	.283	A = 11.0 sq in.; $A_2 = 17$ sq in.; 30° flap.
10	B	.0155	.0017	.078	A = 11.0 sq in.; $A_2 = 0$
11	B	.0155	.0015	.068	A = 11.0 sq in.; $A_2 = 6.8$ sq in.
12	C	.0155	.0017	.078	A = 11.0 sq in.; $A_2 = 0$
13	C	.0157	.0019	.087	A = 11.0 sq in.; $A_2 = 7.4$ sq in.
14	D	.0157	.0019	.087	A = 11.0 sq in.; $A_2 = 0$
15	D	.0157	.0019	.087	A = 11.0 sq in.; $A_2 = 6.8$ sq in.
16	D ₁	.0163	.0025	.114	Juncture cut back 1 1/8 in., A = 11.0 sq in.; $A_2 = 0$
17	D ₂	.0173	.0035	.160	Juncture cut back 2 1/4 in., A = 11.0 sq in.; $A_2 = 0$
18	Dx	.0155	.0017	.078	Scoop entrance moved back 8 in., A = 11.0 sq in.; $A_2 = 0$
19	E	.0223	.0085	.93	No baffle, $A_2 = 0$
20	E	.0210	.0072	.79	No baffle, $A_2 = 6$ sq in.
21	F	.0275	.0137	1.50	No baffle, $A_2 = 0$

TABLE II.- AVAILABLE OVER-ALL PRESSURE DIFFERENCE

Scoop	α (deg)	Front pressure, P_f/q			Rear P_r/q	Exit P_e/q	$\Delta P/q$
		Nose	Lip	Baffle			
A	-2.1	0.51	----	0.58	0.66	-0.22	0.88
	1.1	.58	----	.64	.71	-.18	.89
	8.7	.73	----	.76	.83	-.07	.90
B	-2.1	0.50	0.67	0.58	0.67	0.02	0.65
	1.1	.59	.73	.64	.72	.03	.69
	8.7	.73	.85	.75	.82	.04	.78
C	-2.1	0.51	0.67	0.57	0.65	0.09	0.56
	1.1	.59	.73	.64	.71	.11	.60
	8.7	.73	.84	.75	.81	.16	.65
D	-2.1	0.52	0.60	0.58	0.63	0.02	0.61
	1.1	.63	.69	.65	.71	.02	.69
	8.7	.78	.78	.74	.80	.03	.77

L-331

TABLE III.- PRESSURE DROP ACROSS BAFFLE PLATE

L-331 Scoop	α (deg)	A (sq in.)	A_2 (sq in.)	Front pressure, p_f/q			Rear p_r/q	Exit p_e/q	$\Delta p/q$		
				Nose	Lip	Baffle					
A	-2.1	5.1	3.0	0.54	----	0.60	0.54	----	0.06		
	1.1			.63	----	.67	.59	----	.08		
	8.7			.80	----	.80	.69	----	.11		
	-2.1		6.0	3.0	.55	----	.61	.40	----	.21	
	1.1				.65	----	.68	.45	----	.23	
	8.7				.81	----	.78	.53	----	.25	
	-2.1			17.0 ^a	6.0	.64	----	.67	.19	----	.86
	1.1					.74	----	.75	.16	----	.91
	8.7					.86	----	.79	.08	----	.87
	-2.1	10.2	3.0	.54	----	.59	.61	----	----		
	1.1			.64	----	.66	.67	----	----		
	8.7			.81	----	.77	.78	----	----		
	-2.1		6.0	3.0	.56	----	.61	.57	----	.04	
	1.1				.65	----	.67	.62	----	.05	
	8.7				.84	----	.79	.72	----	.07	
	-2.1			17.0 ^a	6.0	.74	----	.71	.10	----	.61
	1.1					.83	----	.76	.13	----	.63
	8.7					.94	----	.82	.20	----	.62
B	-2.1	10.2	6.8	0.58	0.79	0.64	0.57	0.12	0.07		
	1.1			.70	.85	.71	.63	.13	.08		
	8.7			.83	.90	.80	.68	.15	.12		
C	-2.1	10.2	7.4	0.54	0.74	0.61	0.57	0.24	0.04		
	1.1			.64	.79	.67	.61	.26	.06		
	8.7			.82	.89	.78	.70	.32	.08		
D	-2.1	10.2	6.8	0.58	0.60	0.66	0.55	0.12	0.11		
	1.1			.68	.67	.71	.60	.12	.11		
	8.7			.82	.76	.82	.67	.15	.15		
E	-2.1	Open	6.0	0.70	----	----	0.39	0.05	----		
	1.1			.76	----	----	.48	.10	----		
	8.7			.83	----	----	.58	.16	----		

^aThe 30° flap.

TABLE IV.- SCOOPS FOR MINIMUM DRAG

400 mph - 20,000 ft altitude

(1)	(2)	(3)	(4)	(5)	(6)	(7)	(8)	(9)	(10)	(11)*	(12)*	(13)*		
Example	K	ΔP (lb/ sq ft)	c	C_f	k	Q/F (fps)	$\frac{A_1}{F}$	V_1 (mph)	$\frac{V_1}{V}$	$kC_f \frac{A_1 F}{F S}$	$cK^3 \left(\frac{\Delta P}{q}\right)^{3/2} \left(\frac{F}{A_1} - 1\right)^2 \frac{F}{S}$	C_{D_p}		
1	Intercooler	0.2	60	Sudden exp.	1	1.5	1		0.112	373	0.94	0.0020	0.0009	0.0029
2					1	.79	1		.156	309	.77	.0013	.0006	.0019
3					1	.059	2.4	61.56	.234	179	.45	.0004	.0002	.0006
4					1	.008	2.4		.414	101	.25	.0001	.0000	.0001
5				Grad. exp.	0.13	1.5	1		0.057	734	1.83	0.0010	0.0005	0.0015
6					.13	.79	1		.071	594	1.48	.0007	.0003	.0010
7					.13	.059	2.4	61.56	.123	341	.85	.0002	.0001	.0003
8					.13	.008	2.4		.250	182	.45	.0001	.0000	.0001
9	Radiator	0.5	40	Sudden exp.	1	1.5	1		0.218	392	0.98	0.0039	0.0015	0.0054
10					1	.79	1		.265	323	.81	.0025	.0009	.0034
11					1	.059	2.4	125.6	.430	199	.50	.0007	.0002	.0009
12					1	.008	2.4		.688	125	.31	.0002	.0000	.0002
13				Grad. exp.	0.13	1.5	1		0.115	745	1.86	0.0021	0.0009	0.0030
14					.13	.79	1		.141	608	1.52	.0013	.0006	.0019
15					.13	.059	2.4	125.6	.240	357	.89	.0004	.0002	.0006
16					.13	.008	2.4		.425	202	.50	.0001	.0000	.0001

*Calculated for $F = 2.5$ sq ft and $S = 300$ sq ft.

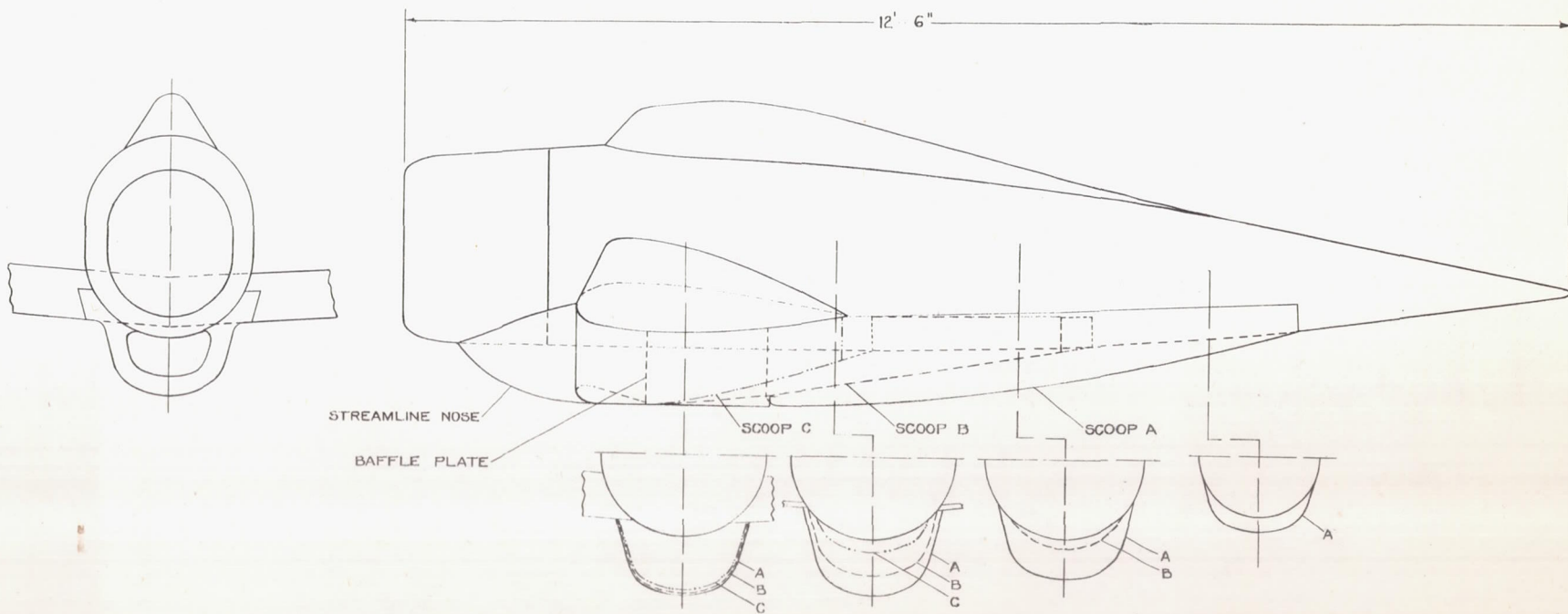


FIGURE 1 - LAYOUT OF TEST ARRANGEMENTS SHOWING SCOOPS A, B, AND C.

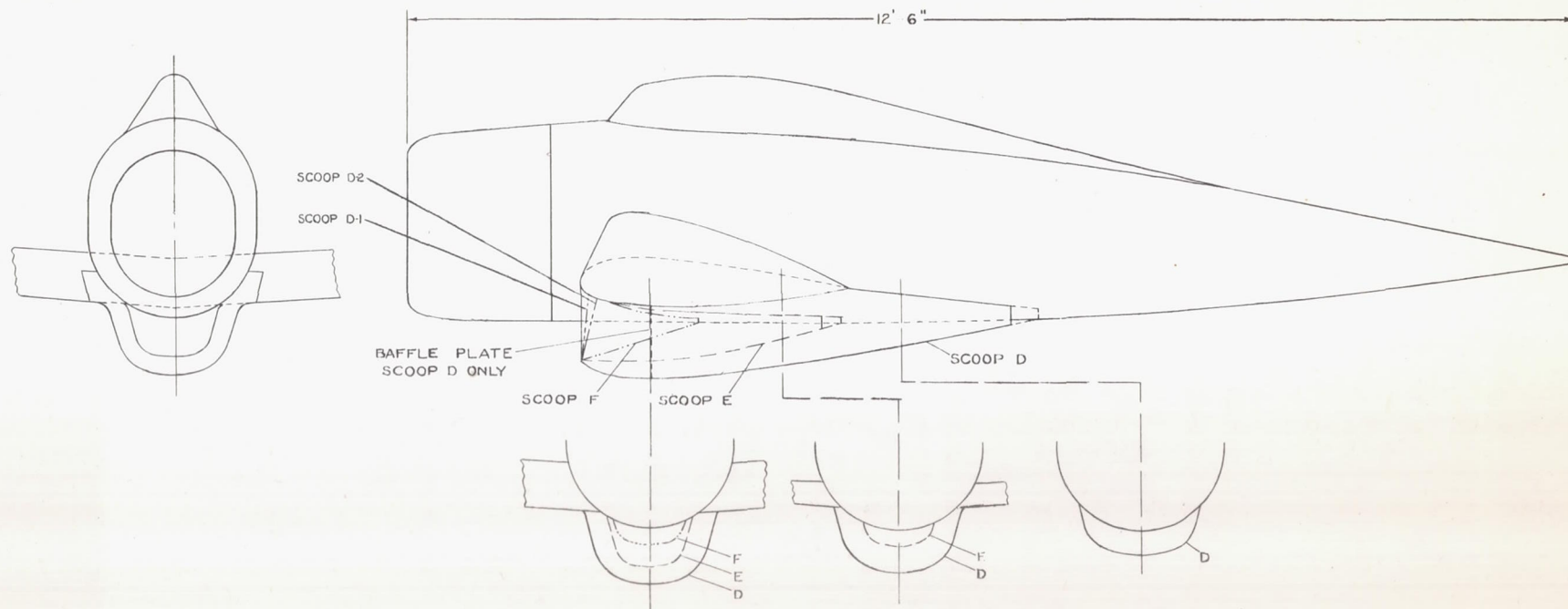


FIGURE 2 - LAYOUT OF TEST ARRANGEMENTS SHOWING SCOOPS D, E, AND F.

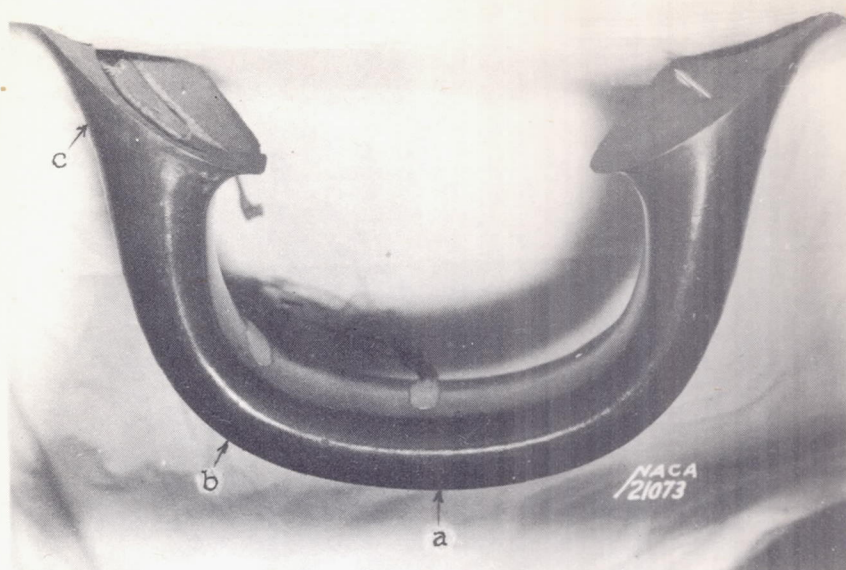


Figure 3.- Nose for scoops A,B, and C. Static pressure orifices at a, bottom center line; b, corner; and c, fillet.

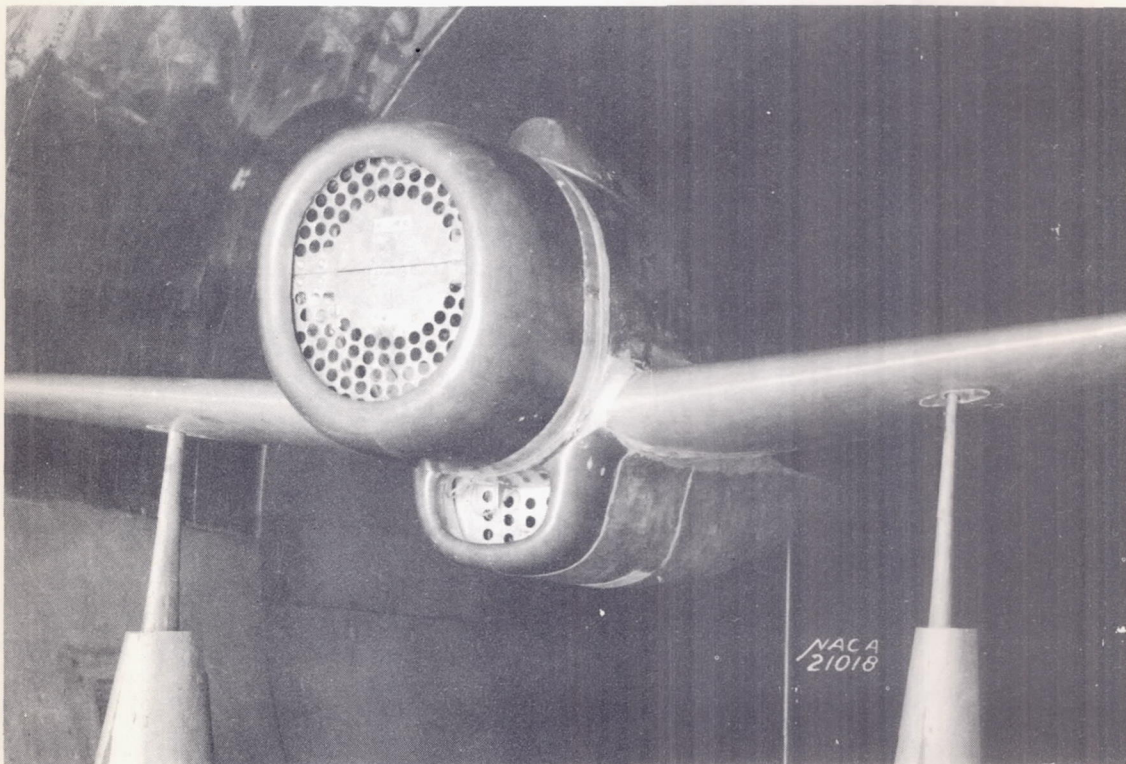


Figure 4.- Model with scoop A, exit closed.

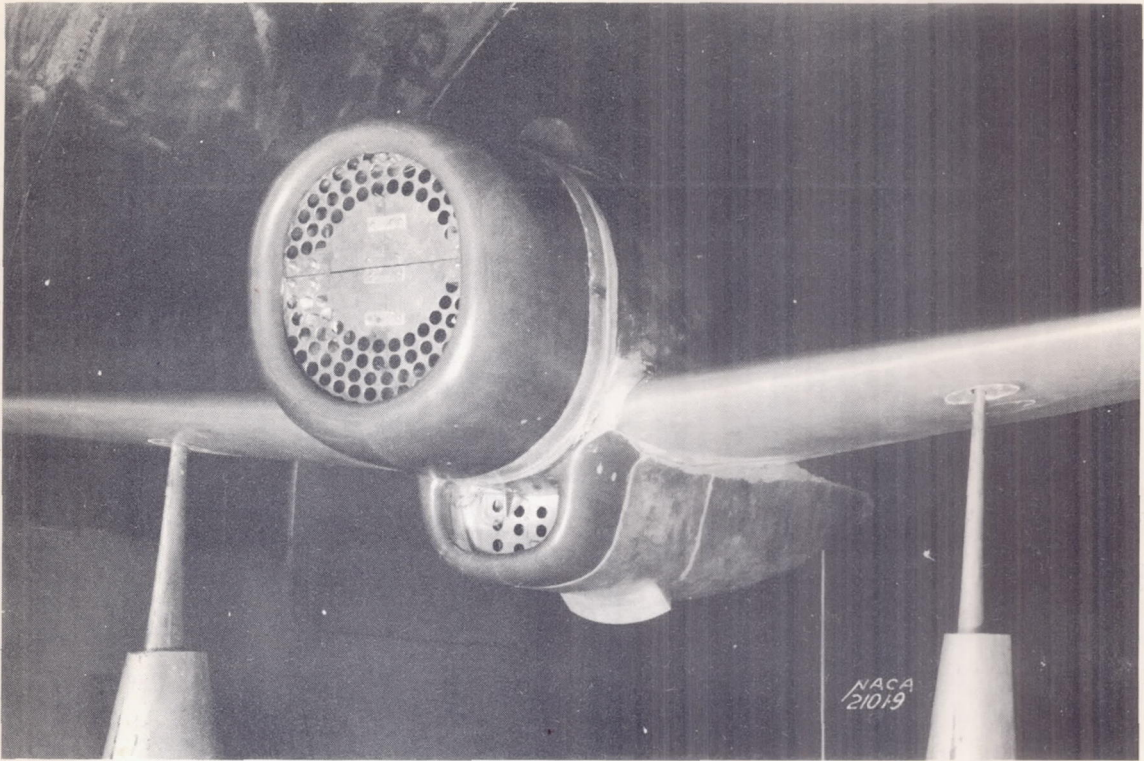


Figure 5.- Model with scoop A, 30° flap.

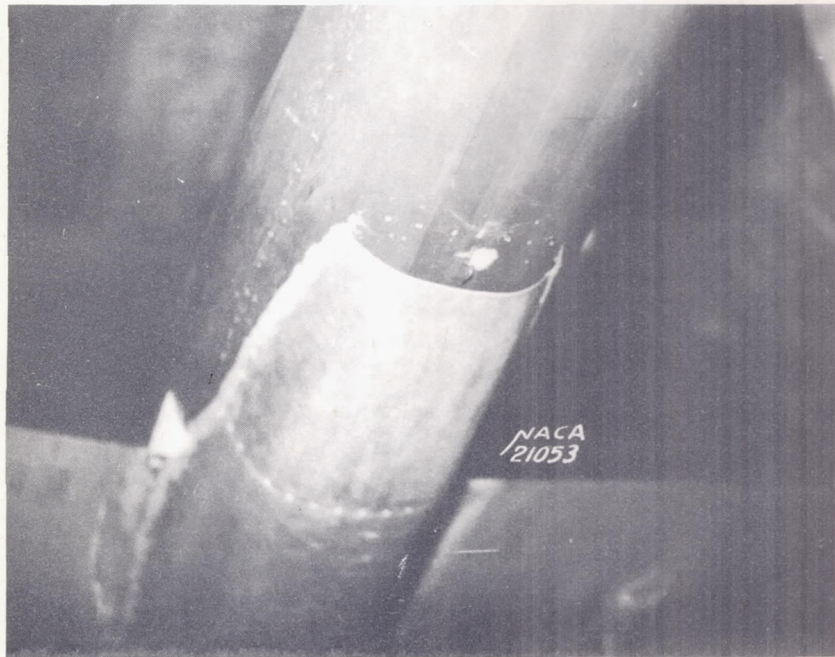


Figure 6.- Exit of scoops B and D.

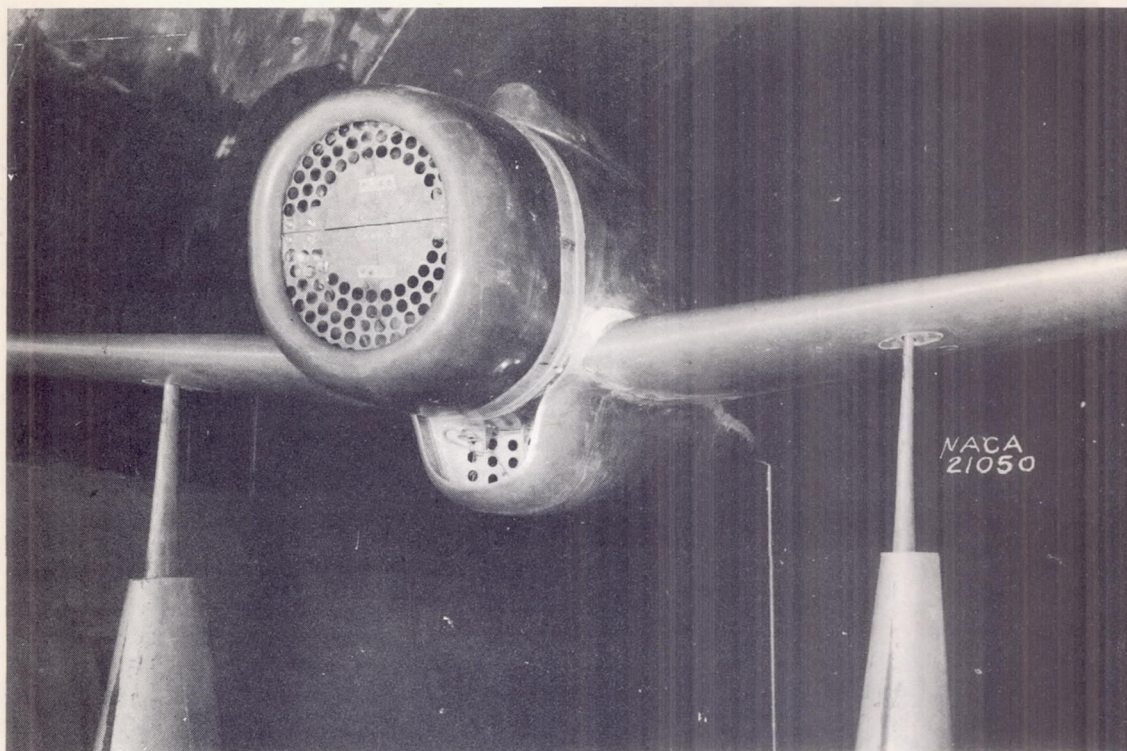


Figure 7.- Model with scoop D, exit closed.



Figure 8.- Model with scoop E, exit open.

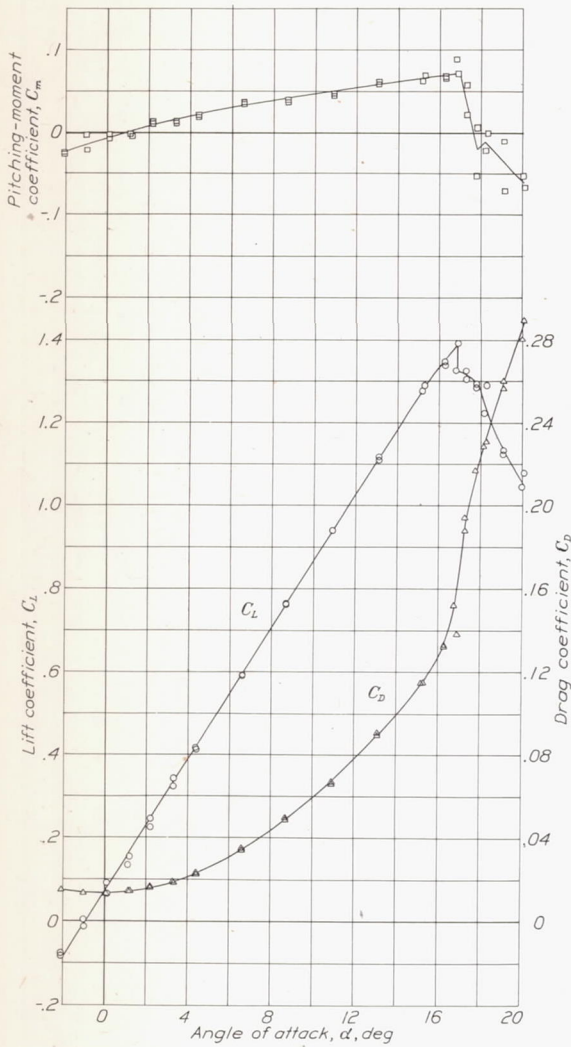


Figure 9.- Force test results on basic model.

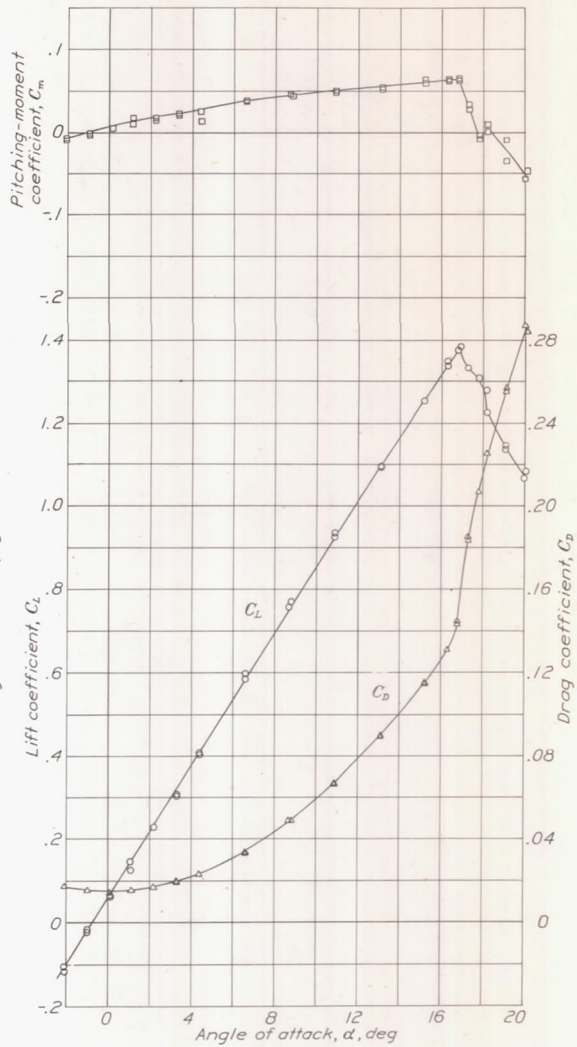


Figure 10.- Force test results on model with scoop B, air flow.

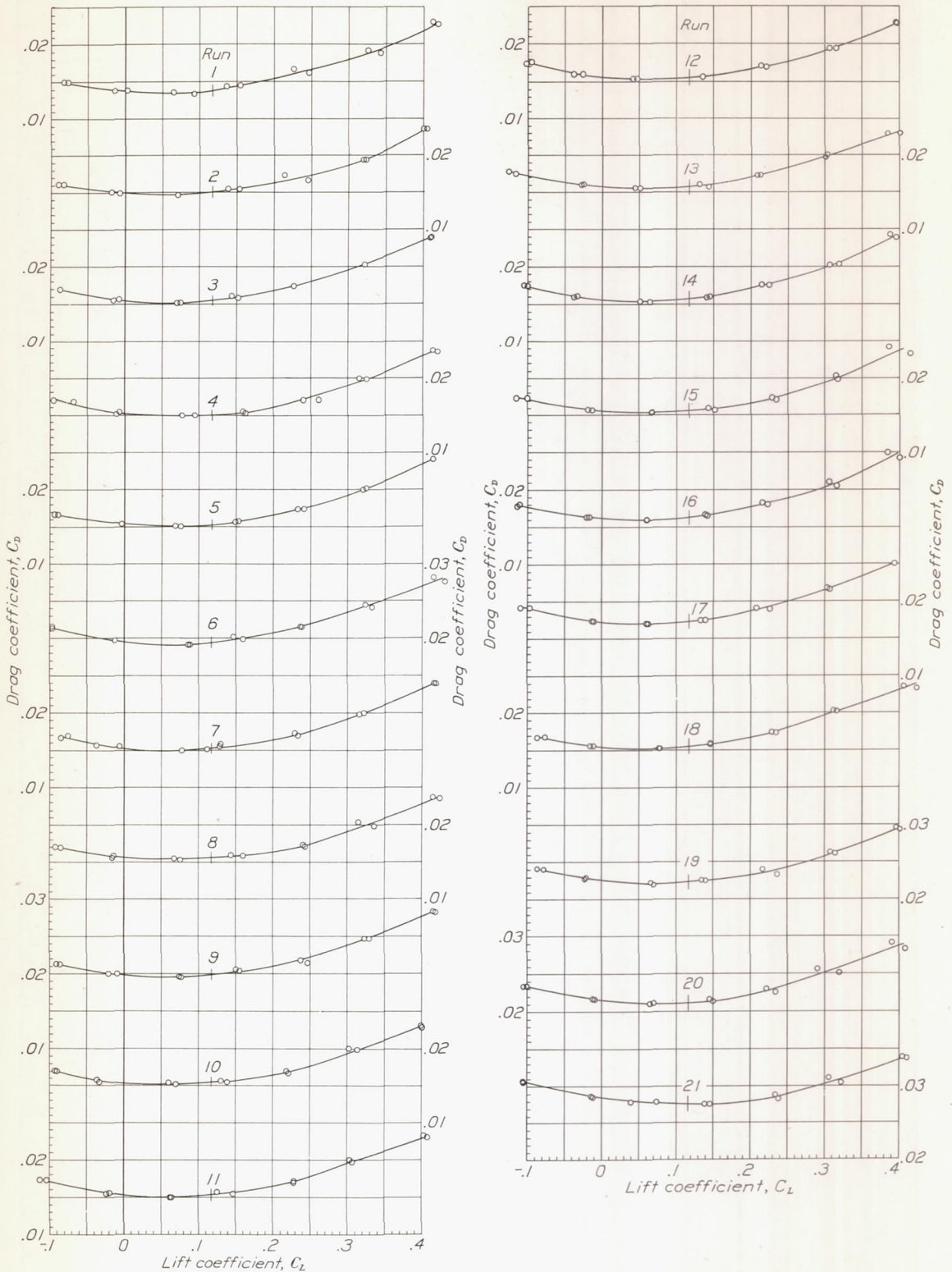
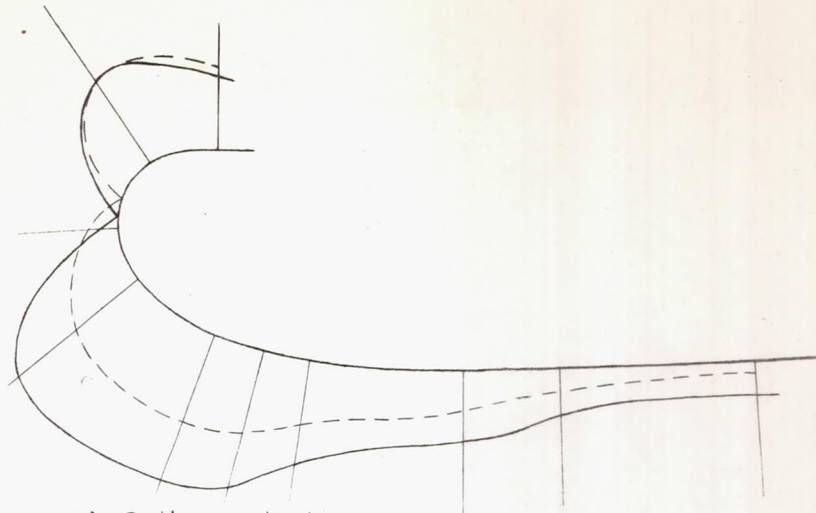
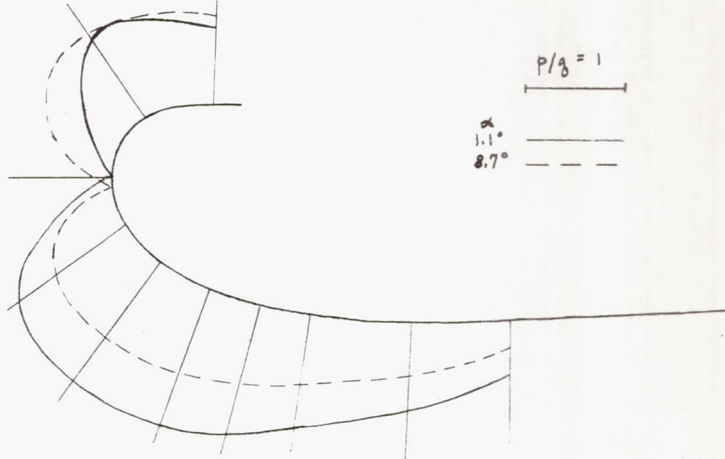


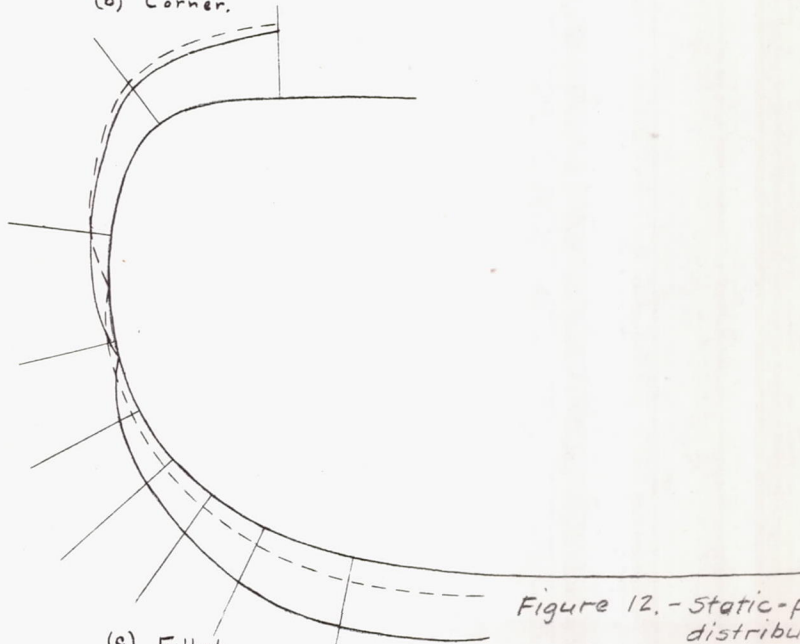
Figure 11.- Polars for the test arrangements.



(a) Bottom, center line.



(b) Corner.



(c) Fillet.

Figure 12. - Static-pressure distribution

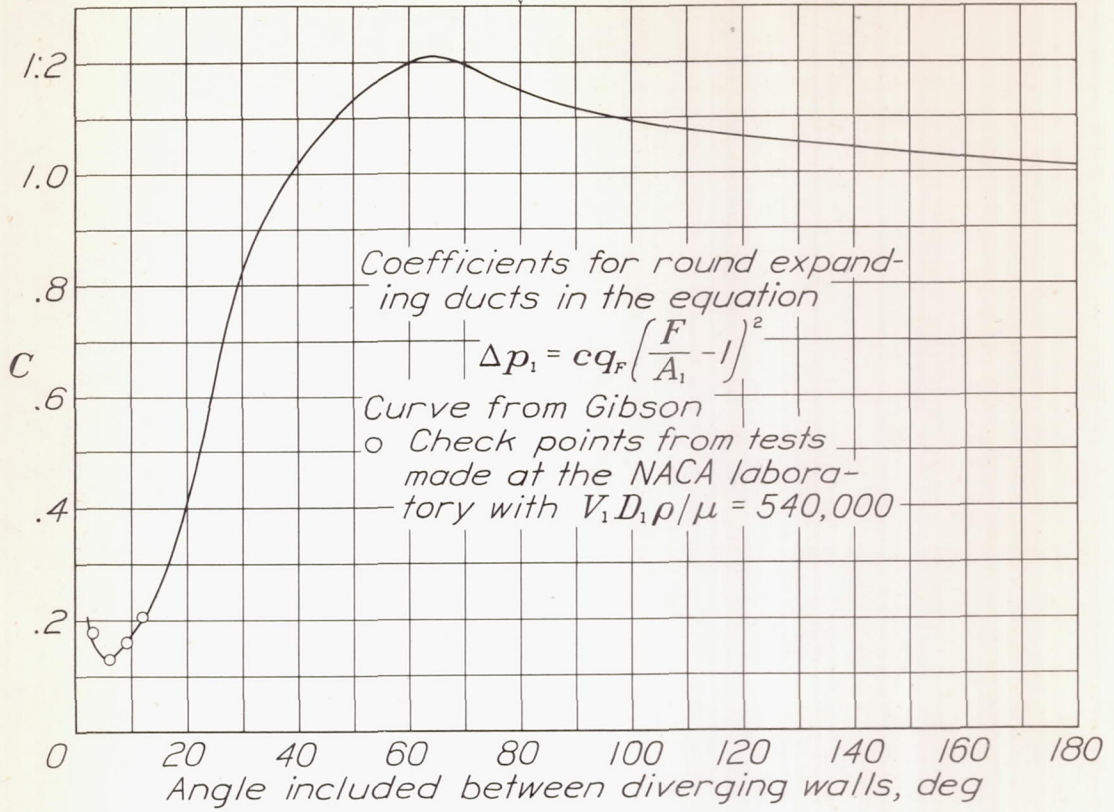


Figure 13.- Chart for determining the coefficient C.

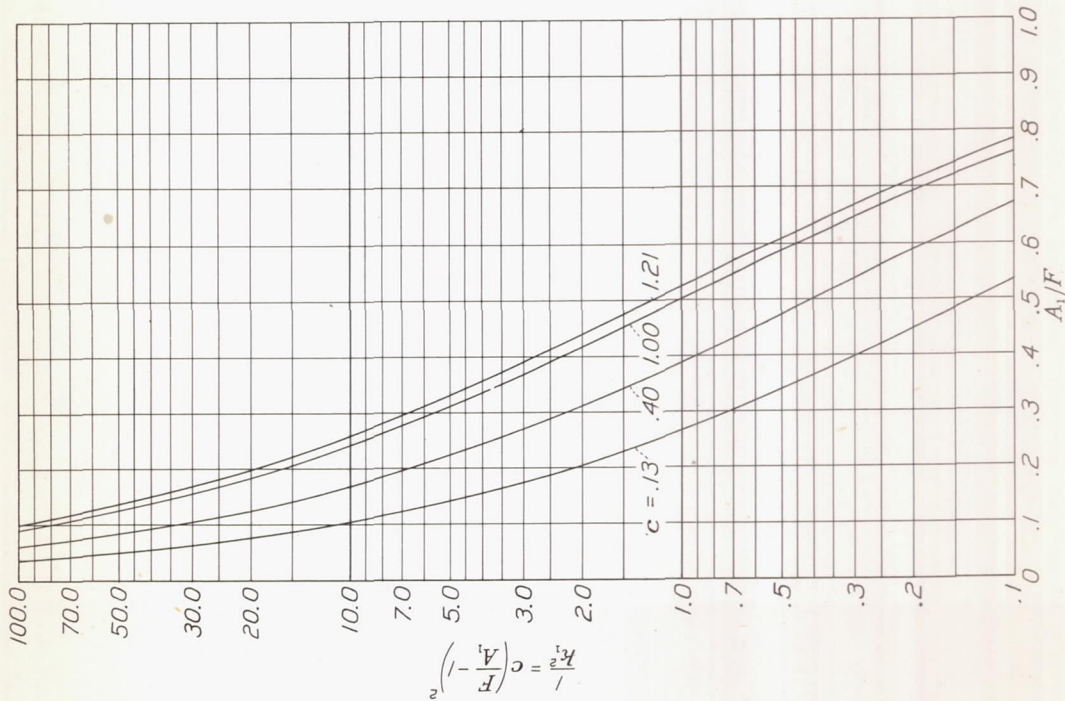


Figure 14.- Chart for determining the entrance conductance.

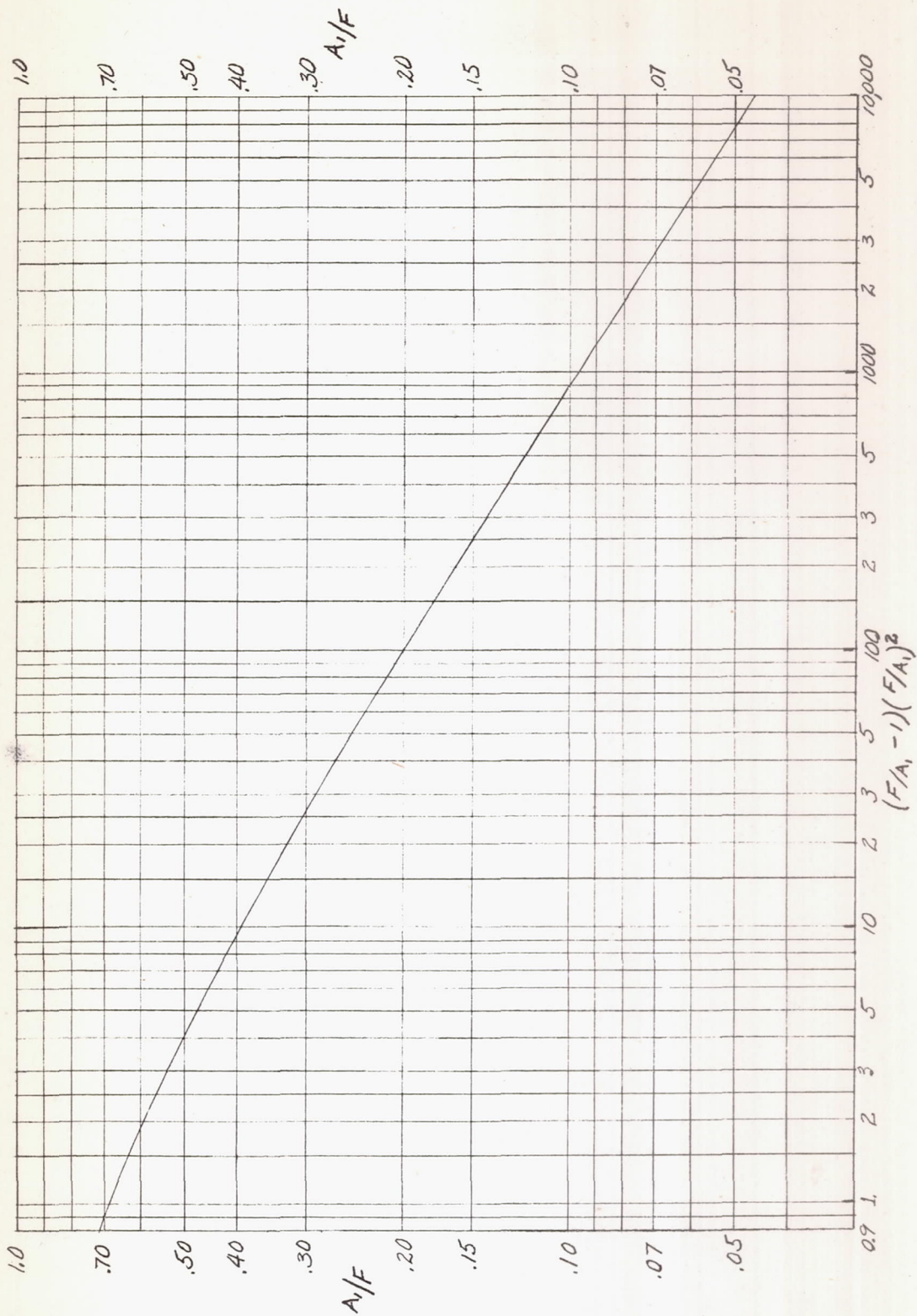


Figure 15. - Chart to determine A_1/F for minimum drag.